J Solid State Electrochem (2012) 16:557–561
DOI 10.1007/s10008-011-1384-x

ORIGINAL PAPER

A high-capacity graphene nanosheet material with capacitive characteristics for the anode of lithium-ion batteries

Tian Li · Lijun Gao

Received: 19 February 2011 / Revised: 7 March 2011 / Accepted: 16 March 2011 / Published online: 12 April 2011

Abstract Graphene nanosheets are prepared from H_2 thermal reduction of graphite oxide at 300 °C. The graphite oxide interlayer has readily been expanded through chemical oxidation of meso-carbon micro-beads graphite raw material. After H_2 reduction, the carbon/oxygen ratio of graphene is increased from that of graphite oxide due to the removal of oxygen-containing functional groups as it is demonstrated from IR spectra. The d-spacing of resulting graphene nanosheets is increased to 0.37 nm, which facilitates lithium intercalation. Such synthesized graphene nanosheet material as anode of lithium-ion battery has exhibited high reversible discharge capacity of 1,540 mAh g^{-1} at a current density of 50 mA g^{-1}, and the coulumbic efficiency was 97% over 50 cycles. The discharge curve of the anode material shows a continuously increased voltage profile, which is a characteristic of a capacitive material.

Keywords Graphene nanosheets · High capacity · Anode · Capacitive characteristics · H_2 reduction

Introduction

Lithium-ion batteries (LIB) have been widely used in portable electronic devices. With recent development of electric vehicles, higher energy density LIBs are demanded as power sources. Silicon and its alloys have been explored as high capacity alternative anode materials to graphite [1, 2]. Graphite has a Li storage capacity of 372 mAh g^{-1} due to limited Li-ion storage sites within sp^2 carbon hexahedrons [3]. Since its discovery in the pioneering work of Novoselov et el [4], graphene was also considered a potential alternative to graphite in LIB. Graphene is composed of two-dimensional layers with one atomic thickness and a high surface area of 2,630 m^2 g^{-1}. It has superior electrical conductivity, outstanding electronic behaviors [5], remarkable mechanical properties [6], and broad electrochemical stability window. Recent studies [7, 8] show that graphene is capable of Li storage with reversible capacity in the range of 500–600 mAh g^{-1}. In the work of Wang et el [9], a specific capacity of 945 mAh g^{-1} for the graphene anode in the initial discharge was reported, and a reversible discharge capacity of 650 mAh g^{-1} was obtained in the following cycles.

The possibility of higher Li-storage capacity was explored by controlling layered structures of graphene. Various attempts have been made in order to create single-layer graphene. These, in general, can be classified into three different routes: namely (1) mechanical peeling; (2) epitaxial growth; and (3) solution-based reduction of graphene oxide. Novoselov et al. [10] produced single graphene sheets using a mechanical peeling method; however, it is very difficult to control the morphology of graphene particles. The epitaxial-grown graphene was prepared by treatment of silicon carbide wafer substrate at high temperatures, and in this technique, the overall quality of the graphene depends largely on the heating temperature of the substrate. The solution-based or chemically modified routes have been widely used in producing graphene in large quantities [11–13]. The graphene can be prepared in two steps: the oxidation of graphite and chemical reduction of graphite oxide (GO). GO is easily exfoliated in water and

T. Li · L. Gao
Department of Chemistry, Nanchang University,
Nanchang 330031, China

T. Li · L. Gao (✉)
School of Energy, Soochow University,
Suzhou 215006, China
e-mail: gaolijun@suda.edu.cn

is strongly hydrophilic, thus, it is formed into stable colloidal dispersion. GO can be fabricated by oxidative treatment of graphite through three methods developed by Brodie [14], Hummers and Offeman [15], and Staudenmaier [16]. Then graphene can be prepared from GO sheets using three different routes including hydrazine reduction, pyrolytic de-oxidation, and electron beam irradiation, and hydrazine reduction has been the most commonly used method [17]. Although hydrazine reduction is an effective way to produce uniform-sized graphene, hydrazine is very toxic, extremely corrosive, and the reaction requires a long time, usually in 24 h. Pan et al. [18] made graphene in a nitrogen atmosphere at 300 °C for 2 h, and the first charge and discharge capacities were 1,544 and 1,013 mAh g^{-1} at a current density of 50 mA g^{-1}. The reversible capacity was kept in the range of 1,013–834 mAh g^{-1} with capacity retention of 82% after 15 cycles.

In this work, graphene nanosheets were prepared by a slow heating process at low temperature using mesocarbon micro-beads (MCMB) graphite as the starting material. GO intermediate was further thermally reduced in H_2/Ar atmosphere at 300 °C. The resulting graphene nanosheet material was examined as anode electrode of Li-ion battery, and it was found that the material is capable of high-capacity lithium storage. To the best of our knowledge, such demonstrated high reversible capacity with hydrogen-reduced graphene nanosheets as anode of Li-ion battery has not been reported previously in the literature.

Experimental

Preparation of GO and graphene nanosheets

First MCMB (5 g) was added into concentrated H_2SO_4 (98%) under stirring in the ice water bath. Then sodium nitrate (2.5 g) and potassium permanganate (15 g) were gradually added into the solution. The mixture was kept at 0 °C for 2 h. The ice water bath was then removed and the temperature of the suspension was brought to 38 °C, where it was maintained for 30 min under stirring. The mixture was further diluted by adding de-ionized (DI) water (230 ml) slowly, causing an increase in temperature to 98 °C. The suspension was maintained at this temperature for 15 min. The suspension was then further diluted to approximately 700 ml with warm DI water and treated with 250 ml of 5% H_2O_2. The product was filtrated and washed with 5% HCl until sulfate could not be detected with $BaCl_2$, and then the resulting GO was dried at 65 °C in a vacuum. GO was thermally reduced in a tube furnace in an Ar/H_2 (10% H_2) atmosphere at 300 °C for 2 h with heating rate of 2 °C min^{-1}.

Measurements

The electrode assembly was made by laminating graphene (80 wt.%), Polyvinylidene fluoride (10 wt.%) and Super-P-Li conductive carbon (10 wt.%) in N-methyl pyrrolidine slurry onto a copper foil (14 μm), dried at 100 °C for 2 h, then the laminate assembly was roll-pressed to a thickness of 40 μm. Disk electrodes of 16 mm diameter were punched out of the laminate sheet and used as working electrode with the weight of active material in the range of 0.90–1.10 mg. Electrochemical test cells were constructed in a glove box (Braun) filled with argon gas, with Li metal as counter electrode and 1.3 M $LiPF_6$ in a 1:3 (mass ratio) mixture of ethylene carbonate and dimethyl carbonate electrolyte. Celgard 2320 membrane was used as separator. The cells were charged and discharged in a voltage range from 0.005 to 3.5 V vs. Li^+/Li at current densities of 50–100 mA g^{-1}. Morphology of the prepared graphene material was examined by scanning electron microscope (SEM) and transmission electron microscope (TEM).

Results and discussion

To investigate the morphology of the products, field emission SEM (FE-SEM) images were taken for the graphene sample. Figure 1a, b reveal that the original graphite material is already exfoliated into folded layers, and the layered platelets are composed of curled graphene nanosheets. GO and graphene samples were measured by X-ray energy dispersive analysis (EDAX) in FE-SEM chamber. The carbon to oxygen (C/O) atomic ratio of GO is measured to be 89.55:10.45, while for graphene, it is 99.19:0.81.

The structural changes from GO to graphene were investigated by IR spectroscopy as shown in Fig. 2. The patterns of GO exhibits a characteristic peak of carbonyl groups (C=O, ca. 1,700 cm^{-1}). After de-oxidation, the peak of C=O in graphene disappeared, implying that the oxygen atoms are mostly removed. The EDAX results illustrate that the C/O atomic ratio increased rapidly after H_2 treatment at low temperature, which is also supported by the disappearance of the oxygen-containing group from the IR spectra.

The high-resolution TEM (HRTEM) and TEM analyses for the products were also used to elucidate the structure features of GO and graphene nanosheets. The HRTEM image in Fig. 3a revealed a regularly layered structure of GO, which is very similar to that of graphite. However, from the reading of red bar distance (5.0 nm corresponding to 14 counts of layers) in Fig. 3a, it is calculated that the d-spacing between two GO layers is about 0.357 nm, which is larger than that of graphite (0.335 nm), indicating that GO

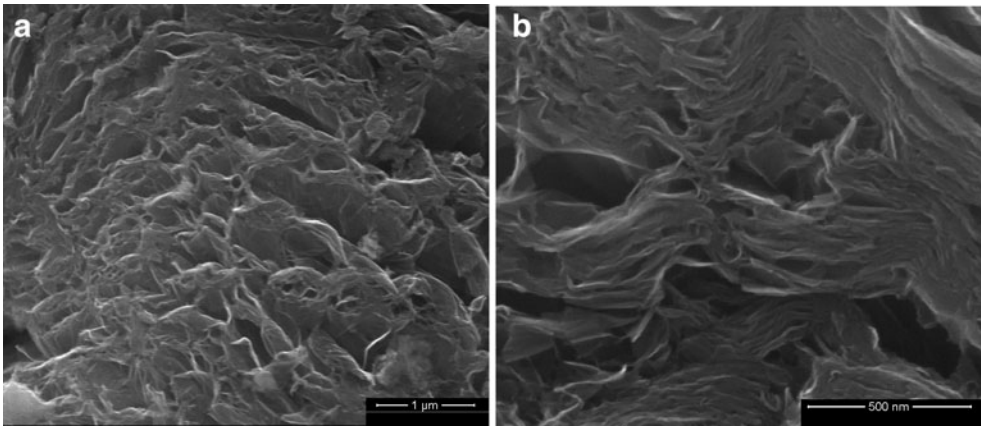

Fig. 1 FE-SEM observation of thermally H_2 reduced graphene material: **a** low-magnification SEM image of loose graphene sheets; **b** high-magnification SEM image of graphene sheets

interlayer distance has increased about 6.5% after oxidation reaction. As it is seen in Fig. 3b, the HRTEM image of graphene nanosheets exhibited altered structure from GO. The graphene is also layer structured; however, it is irregular and folding. The de-oxidization reaction by H_2 at low temperature makes the disruption of planar sp^2 carbon sheets by the introduction of sp^3-hybridized carbon, and the two-dimensional carbon sheets evolves into disordered and entangled sheets through re-arrangement. From Fig. 3b, it is seen that the red bar length is about 1.85 nm (five counts of layers), so the d-spacing between two graphene nanosheets is estimated to be 0.37 nm. These graphene nanosheets are entangled with each other and resemble crumpled paper as shown in the TEM image of Fig. 3c. Figure 3c shows disordered graphene layers, which are made of carbon sheets stacked in tens of atomic layers.

Figure 4a shows the first two charge–discharge voltage profile of graphene electrode vs. Li^+/Li in the voltage range of 3.5–0.005 V at the current density of 50 mA g^{-1}. The first charge curve for the graphene electrode shows a plateau at about 1.4 V representing the solid electrolyte interface (SEI) formation, which causes the loss of capacity that is irreversible. However, this plateau does not exist in the second cycle profile implying that the intercalation reaction has become reversible starting from the second cycle. No distinct lithium intercalation voltage plateau can be observed for the graphene material after the SEI formation, which differs from graphite anode where voltage plateau typically appears at 0–1.0 V. This behavior of graphene nanosheets is similar to that of hard carbon [19], possibly due to the common nature of these two carbon materials that have expanded d-spacing layers and less extent of crystallization than graphite. Similar behavior can also be observed in the work of references [7–9]. It is seen in the discharge curve that the majority contribution of capacity is in the region above 1.0 and up to 3.5 V, the voltage continuously increases under constant current discharge, this is typically characteristic of a capacitive material. For hard carbon anode though, the discharge capacity mostly appears in the voltage range of 0.05 to 1 V [19], and above 1 V, the voltage increases dramatically with little capacity contribution. In this aspect, the graphene material can be distinguished from hard carbon in discharge profile. If the graphene anode couples with a Li-ion battery cathode material such as $LiFePO_4$, the discharge curve of the cell will show a declined voltage profile from starting voltage (possibly 3.2 V) all the way to 0 V. Such a cell may also be considered a hybrid capacitor/battery, which involves half capacitive electrode and half battery electrode. One advantage of such a cell is the possibility of clear indication of state of charge from the reading of cell voltage.

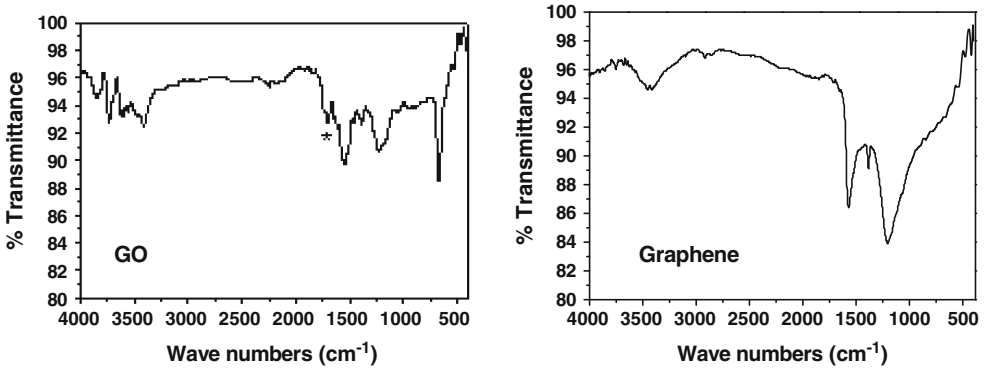

Fig. 2 IR spectra of GO and graphene (region 400–4,000 cm^{-1})

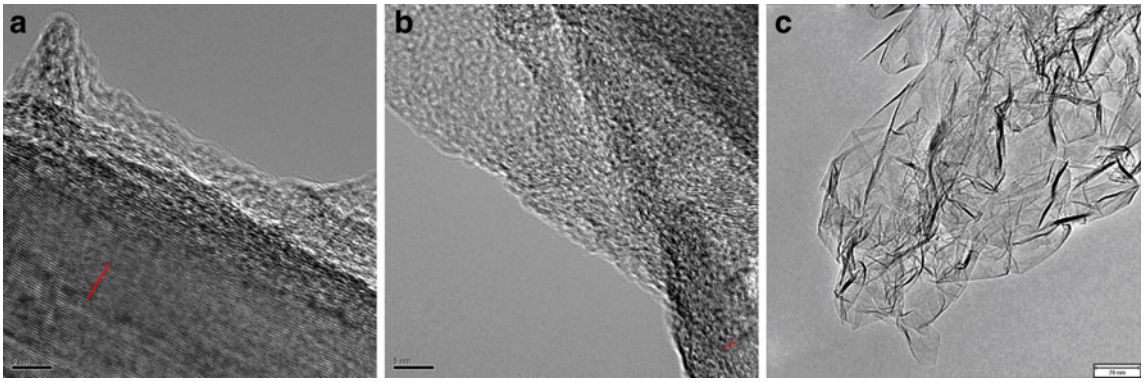

Fig. 3 **a** HRTEM image of GO (scale bar length 5 nm), **b** HRTEM image of graphene nanosheets (scale bar length 5 nm), and **c** TEM image of graphene nanosheets (scale bar length 70 nm)

It is shown in Fig. 4a that the first charge and discharge capacities of the graphene electrode are 2,274 and 1,633 mAh g^{-1}, respectively, at the current density of 50 mA g^{-1}. The weight in calculation is based on the graphene active material. The high irreversible capacity of graphene electrode in the first cycle could be explained from the formation of SEI film. The 2,274 mAh g^{-1} capacity in charge is close to the theoretical value of lithium storage in LiC, where Li:C=1:1. The formation of SEI film consumes a lot of lithium ions in the first cycle leading to a high capacity loss (2,274–1,633=641 mAh g^{-1} corresponding to 28% inefficiency, which is much higher than that of a graphite anode). Higher surface area of the graphene material could be the major reason accounting for the initial capacity loss. The second charge and discharge capacities are 1,618 and 1,540 mAh g^{-1}, respectively, this small amount of capacity loss (about 5%) indicates that starting from second cycle lithium intercalation/de-intercalation processes become rather reversible. Even with the initial capacity loss of 28% on SEI formation due to the high surface area of graphene nanosheet material, the reversible discharge capacity of 1,540 mAh g^{-1} obtained in the second cycle is still considered the highest value reported so far, which makes the graphene nanosheet a proper anode material of Li-ion battery. The key to the high reversible capacity is the treatment of graphite oxide by thermal H_2 reduction which removed the oxidative surface functional groups in graphene nanosheets synthesis. Facile lithium ion deintercalation occurs in the periodically layered region and expanded interlayers of graphene material during shallow delithiation process, and the extraction of lithium ions from interlayer nanovoids contributes the most to the high capacity in the deep delithiation stage [20], while the voltage continues to increase in discharge process.

Figure 4b illustrates the cycle performances of graphene electrodes at current densities of 50 and 100 mA g^{-1}. Coulombic efficiency in relation to cycle number at the current density of 50 mA g^{-1} is also displayed. It is seen that after the first irreversible cycle, the discharge capacity value from the second to the 50th cycle changes insignificantly, with a reversible capacity retention of 79.4% at 50th cycle comparing to that of the second cycle. Figure 4b reveals that the graphene material has a very stable cycle coulombic efficiency of over 97% (except the first cycle) at the current density of

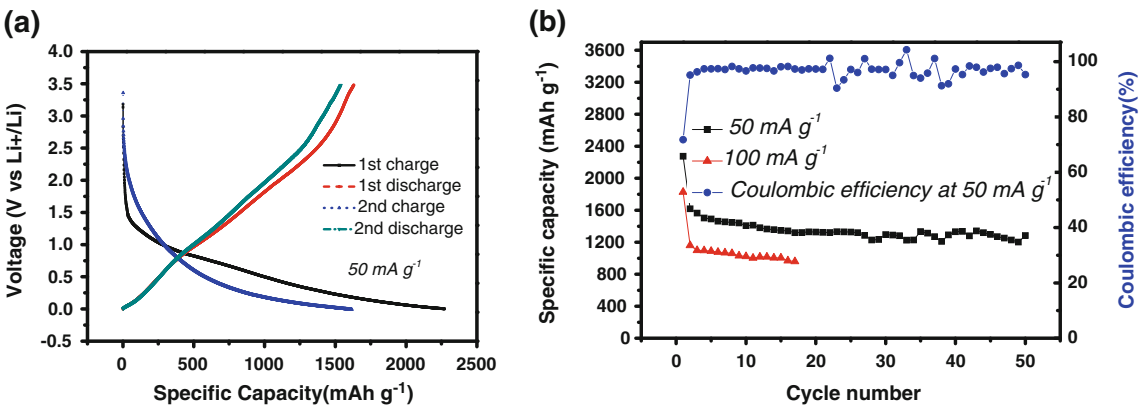

Fig. 4 **a** First two charge–discharge curves of graphene nanosheet electrode at current density of 50 mA g^{-1}; **b** cycle performance of graphene electrodes at current densities of 50 and 100 mA g^{-1} and coulombic efficiency in relation to cycle number at current density of 50 mA g^{-1}

50 mA g^{-1}. At higher rate of 100 mA g^{-1}, the discharge capacity changes from 1,160 to 958 mAh g^{-1} from the second to the 16th cycles. The results show that the graphene material has superior lithium intercalation/deintercalation property with capacitive characteristics.

Conclusions

Graphene nanosheet material was prepared from thermal reduction of GO by H_2 at 300 °C which removed surface functional groups (carbonyl groups) from GO. This method of thermal H_2 reduction also resulted in converting non-conducting GO into highly conductive graphene and ordered GO into disordered graphene nanosheets. The graphene interlayer d-spacing was expanded to 0.37 nm through initial exfoliation comparing to that of graphite at 0.335 nm, which has increased by 10% after reaction. The disappearance of oxygen-containing functional group and the increase of d-spacing facilitate more reversible lithium intercalation into graphene layers, thus resulting in higher lithium storage capacity. After the formation of SEI film in the first cycle which is rather compact and stable, reversible intercalation happens in the second cycle. The H_2 reduction "cleaned" graphene nanosheet material exhibits high reversible discharge capacity of 1,540 mAh g^{-1} (second cycle) for lithium deintercalation at a current density of 50 mA g^{-1}. The graphene material also shows high coulombic efficiency at average of 97% through 50 cycles. The behavior of the graphene anode is a characteristic of a capacitor material showing increased voltage profile during discharge.

Acknowledgments Support of this work by Natural Science Foundation of China (No.20663005) is greatly acknowledged.

References

1. Kasavajjula U, Wang C, Appleby AJ (2007) J Power Sources 163:1003–1039
2. Chan CK, Peng H, Liu G, McIlwrath K, Zhang XF, Huggins RA, Cui Y (2008) Nat Nano 3:31–35
3. Ng S-H, Wang J, Wexler D, Konstantinov K, Guo Z-P, Liu H-K (2006) Angew Chem Int Ed 45:6896–6899
4. Novoselov KS, Geim AK, Morozov SV, Jiang D, Zhang Y, Dubonos SV, Grigorieva IV, Firsov AA (2004) Science 306:666–669
5. Novoselov KS, Geim AK, Morozov SV, Jiang D, Katsnelson MI, Grigorieva IV, Dubonos SV, Firsov AA (2005) Nature 438:197–200
6. Hernandez Y, Nicolosi V, Lotya M, Blighe FM, Sun Z, De S, McGovern IT, Holland B, Byrne M, Gun'Ko YK, Boland JJ, Niraj P, Duesberg G, Krishnamurthy S, Goodhue R, Hutchison J, Scardaci V, Ferrari AC, Coleman JN (2008) Nat Nano 3:563–568
7. Yoo E, Kim J, Hosono E, Zhou H-s, Kudo T, Honma I (2008) Nano Lett 8:2277–2282
8. Paek S-M, Yoo E, Honma I (2008) Nano Lett 9:72–75
9. Wang G, Shen X, Yao J, Park J (2009) Carbon 47:2049–2053
10. Novoselov KS, Jiang Z, Zhang Y, Morozov SV, Stormer HL, Zeitler U, Maan JC, Boebinger GS, Kim P, Geim AK (2007) Science 315:1379
11. Stoller MD, Park S, Zhu Y, An J, Ruoff RS (2008) Nano Lett 8:3498–3502
12. Geng Y, Wang SJ, Kim J-K (2009) J Colloid Interface Sci 336:592–598
13. Stankovich S, Piner RD, Nguyen ST, Ruoff RS (2006) Carbon 44:3342–3347
14. Brodie BC (1860) Ann Chim Phys 59:466–472
15. Hummers WS, Offeman RE (1958) J Am Chem Soc 80:1339
16. Staudenmaier L (1898) Ber Dtsch Chem Ges 31:1481–1487
17. Stankovich S, Dikin DA, Piner RD, Kohlhaas KA, Kleinhammes A, Jia Y, Wu Y, Nguyen ST, Ruoff RS (2007) Carbon 45:1558–1565
18. Pan D, Wang S, Zhao B, Wu M, Zhang H, Wang Y, Jiao Z (2009) Chem Mater 21:3136–3142
19. Sun H, He HM, Ren JG, Li JJ, Jiang CY, Wan CR (2007) Electrochim Acta 52:4312–4316
20. Nagao M, Pitteloud C, Kamiyama T, Otomo T, Itoh K, Fukunaga T, Tatsumi K, Kanno R (2006) J Electrochem Soc 153(5):A914–A919